Estimation of Air Leakage Sizes in Building Envelope using High-Frequency Acoustic Impulse Response Technique

Benedikt Kölsch*[1], Björn Schiricke[2], Jacob Estevam Schmiedt[3], and Bernhard Hoffschmidt[3]

1 German Aerospace Center (DLR)
Institute of Solar Research
Karl-Heinz-Beckurts-Str. 13
52428 Jülich, Germany
Corresponding author: benedikt.koelsch@dlr.de

2 German Aerospace Center (DLR)
Institute of Solar Research
Linder Höhe
51147 Cologne, Germany

3 German Aerospace Center (DLR)
Institute for the Protection of Terrestrial
Infrastructures
Linder Höhe
51147 Cologne, Germany

ABSTRACT

Heating energy in buildings represents a significant proportion of the total global energy consumption. Uncontrolled airflow through the building envelope contributes significantly to its energy losses.

Existing methods, like the fan pressurisation technique, which measure the air infiltration rate and quantify individual leakage sizes in buildings, are expensive and time-consuming. Additionally, the accurate detection of the leak location with these methods depends strongly on the experience of the respective building inspector. Moreover, it is hardly possible to identify the size of each leakage accurately and quantify their contributions to the entire building air change rate. Thus, the development of a new measurement method is a vital step.

In this paper, a high-frequency acoustic method is proposed to identify leakage sizes. Using an impulse response technique with multiple microphones and a high-frequency broad-band excitation signal enables the identification of frequency components which are predominantly attenuated inside walls. In a laboratory test chamber, different interchangeable walls have been used. Therefore, it was possible to investigate different leakage sizes and compare them directly in a controlled environment. As an excitation signal, an exponential sine sweep is used, which is able to cover a broad frequency range and simultaneously only excites the desired frequencies. By analysing the spectra, it is possible to differentiate between different cracks and leak sizes. Therefore, this technique has the potential to concentrate only on significant leaks during a building renovation and save building owners time and costs.

KEYWORDS

Air leakage, acoustics, high frequency, impulse response, leakage size

1   INTRODUCTION

Climate protection and environmental degradation have arisen as salient topics nowadays. The building sector is responsible for more than one-third of the global energy consumption and is, therefore, the largest end-use sector (International Energy Agency, 2013). Besides thermal conduction, uncontrolled air infiltration is the main source of increased energy consumption in residential and commercial buildings and, thus, of higher costs for the owners. Emmerich et al. predicted in their research, that airtight houses in the U.S. can potentially

save heating and cooling energy cost in the range from 4 % to 36 % per year (Emmerich et al., 2005). Additionally, unwanted airflow through the building envelope may lead to an impairment of indoor air quality and condensation of moisture inside walls, in particular during winter (TenWolde, 1994).

In order to quantify the airtightness of buildings, typically the fan pressurization method ("blower door test") is applied in buildings (Norm DIN EN ISO 9972). Although this test is applicable to quantify the airflow rate mostly at a pressure difference of 50 Pa between indoor and outdoor, it does not serve the purpose to determine airflow under natural condition. The pressure difference of 50 Pa is often used because it is low enough for most blower door configurations to achieve and high enough to be independent of weather influences outside (Sherman and Chan, 2004).
A less frequently consulted method is the tracer gas dilution method (Norm DIN EN ISO 12569). A non-reactive tracer gas will be released inside a room, and the distribution of the gas throughout the room will be monitored. This method is complex and requires a high standard of measurement equipment. Both methods are expensive and time-consuming. Additionally, it is demanding to find the location of the leaks correctly using these methods. One can use smoke sticks to visualize the airflow or consider the additional usage of infrared cameras to identify different air temperature layers. However, the use of infrared cameras requires a significant temperature difference between indoor and outdoor. Moreover, both methods do not provide information about leakage shape and size.

In this paper, we propose a new method using a high-frequency impulse response technique to identify leakage sizes. Acoustic waves take the same paths as air does, and therefore, it is possible to monitor the way the wave takes. The presented work is part of an ongoing research project to make remote-sensing techniques applicable for energy analysis of existing buildings (Estevam Schmiedt et al., 2017). The goal of this project is to develop a toolbox of measurement and analysis methods to determine the thermal properties of buildings and collect crucial information about the building structure.

2   METHODS

The objective of this work is to identify different leak sizes in different materials of the wall. In order to achieve this, the frequency-dependent sound insulation of different walls is determined. The sound insulation between two rooms can be measured using the sound reduction index R (Norm DIN EN ISO 12354-1):

$$R = \Delta L_P + C = \Delta L_P + 10\lg\left(\frac{S}{A}\right) = \Delta L_P + 10\lg\left(\frac{S}{0.163\dfrac{V}{T}}\right) \tag{1}$$

Here, ΔL_P is the measured sound pressure level difference in dB between two rooms. The sound reduction index can usually not be directly determined by measuring only the sound pressure level difference. In the receiving room, the measured sound pressure is superimposed by reflected sound waves of the surrounding surfaces (Lerch et al., 2009). This fact is considered by the term C of the equation. Here, S is the area of the common partition in m², and A is the equivalent absorption area of the receiving room in m². The equivalent absorption area can be approximated using Sabine's formula, where V is the volume of the receiving room in m³ and T is the reverberation time in seconds which has to be measured in the receiving room. The reverberation time is the time it takes to reduce the energy density to the

one-millionth of the original sound or respectively the time it takes for the sound pressure level to drop 60 dB after the abrupt ending of a generated test signal (Müller and Möser, 2004).

In practice, this formula is usually acceptable and a sufficient approximation of the sound reduction index if rooms are small and the considered frequencies low. However, in this work, higher frequencies are considered as well. Hence, this formula should be adapted, and the air absorption has to be taken into account using the intensity attenuation coefficient m in 1/m:

$$R_A = \Delta L_P + C_A = \Delta L_P + 10\lg\left(\frac{S}{V\left(\dfrac{0.163}{T} - 4m\right)}\right) \tag{2}$$

The attenuation coefficient depends on the frequency, the ambient atmospheric temperature, and the relative humidity and is calculated according to ISO 9613-1 (Norm ISO 9613-1) and Wenmaekers (Wenmaekers et al., 2014). This coefficient increases with increasing ambient temperature and frequency.

2.1 Experimental Setup

In order to be able to compare different materials and leakage sizes under laboratory conditions, a test chamber has been constructed. This chamber consists of two equal sized cells with the following dimensions for each cell: 30.0 cm x 43.5 cm x 31.0 cm. As test specimen replaceable acrylic glass, as well as plywood walls, are used. Each barrier contains an orifice with a diameter of 4, 6, 8 or 10 mm. These orifices simulate potential air leakages inside a wall. Except for these intentional openings, the walls are sealed so that they are airtight.

An ultrasonic omnidirectional dynamic speaker with a frequency range of 1 – 120 kHz is placed in one cell. Two ultrasonic microphones are sited in the test chamber as well, one in each cell. The microphones are 1/4" condenser microphones with an even frequency response and a recommended frequency range of 0.004 – 100 kHz. The signal is generated and evaluated using a python script, and the data acquisition is performed by a USB wide dynamic range signal analyser with a sampling frequency of 216 kHz per channel.

2.2 Measurement Procedure

The calculation of the sound reduction index R_A requires a measurement of the sound pressure level difference ΔL_P and C_A. According to DIN EN ISO 18233 (Norm DIN EN ISO 18233), the sound pressure level difference between two rooms can be calculated using the ratio of the integrated and squared impulse response h of the sending (index 1) and receiving room (index 2):

$$\Delta L_P = 10\lg\left(\frac{\displaystyle\int_0^\infty h_1^2(t)\,dt}{\displaystyle\int_0^\infty h_2^2(t)\,dt}\right) \tag{3}$$

Assuming, the acoustics of a room is a linear and time-invariant system, the entire information of the room transfer function is contained in the room impulse response. Unfortunately, in reality, the system is not perfectly linear, because a measured impulse response contains artefacts caused by noise and the non-linear behaviour of, e.g. amplifiers or transducers. To overcome this problem, a method based on Farina (Farina, 2000) is applied in this paper. Here, an exponential sine sweep with constant amplitude is used as an excitation signal. The excitation signal was generated using a python script and is then recorded in the sending, as well as in the receiving room (see Figure 1). To obtain the desired impulse response, the recorded signal $y(t)$ has to be convolved with an inverse filter signal:

$$h(t) = y(t) * ESS^{-1} \tag{4}$$

In practice, the inverse filter signal ESS^{-1} is the reversed time signal of the exponential sine sweep with modulated amplitude in order to compensate the exponentially changing sweep energy. In contrast to other methods employed for measurement of the impulse response (e.g., the maximum length sequence method or the linear sweep method), the accumulation of nonlinearities in the measured signal can be entirely separated from the actual linear room impulse response using this method. Moreover, the signal-to-noise ratio and the repeatability of the measurements (also with the presence of air and temperature fluctuations) are better than for the other methods. Additionally, the use of an exponential sweep enables the user to consider only relevant frequency bands. In this case, the frequency range is 1−100 kHz. All frequency dependent parameters are finally band filtered and evaluated within a 1/3 octave band (Third-octave filter: TF).
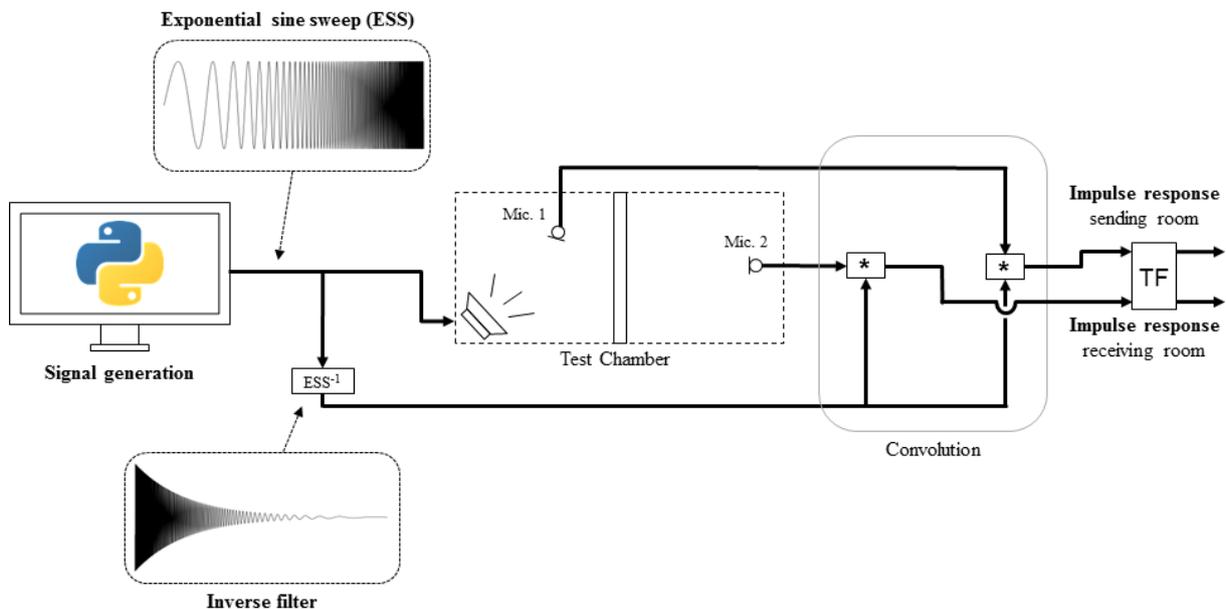

Figure 1: Measurement procedure

Next, the missing parameters for the second part of equation (2) have to be identified. The area of the common partition S and the room volume of the receiving room V are only geometrical parameters and constants. The reverberation time t is frequency dependent and has been measured in the receiving room according to DIN EN ISO 3382-2 (Norm DIN EN ISO 3382-2). In this procedure, the impulse response is measured similar to the method illustrated in Figure 1 in the receiving room for an acrylic glass and a plywood wall in order to calculate the reverberation time. After the impulse responses are 1/3 octave filtered, decay curves are determined for each frequency band by calculating the backwards integration of the squared impulse responses. Subsequently, the sound level can be calculated from the

integrated squared impulse responses, and it is possible to determine the time the sound pressure level takes to drop by 60 dB, which is the reverberation time t_{60}. This process is shown in Figure 2.
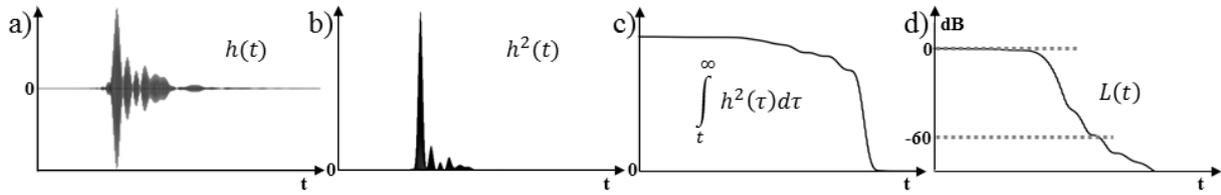

Figure 2: Measurement process of reverberation time: a) Measured impulse response in the receiving room, b) Squared impulse response, c) Backwards integration of the squared impulse response, d) Estimation of reverberation time from sound level $L(t)$ drop

3 RESULTS

In this paper, the sound reduction indexes between the two rooms, as well as the required reverberation times in the receiving room have been measured, which are presented in the following section.

3.1 Reverberation Time Measurements

The measured values of the reverberation time t_{60} in the receiving room for a separation wall of acrylic glass and plywood are shown in Figure 3. As stated above, t_{60} is the time span it takes until the sound pressure level in a room decreases by 60 dB. In practice, the t_{60} is often not measured directly because background noise would distort the measurement. Here, the measurements of the t_{30} and t_{20} have been taken and subsequently extrapolated to the required t_{60} value.

It can be seen that the reverberation time using the acrylic glass wall is higher than the reverberation time using the plywood wall for every frequency. The difference is mainly significant for lower frequencies. For high frequencies, the differences are marginal. The lower reverberation times for a plywood wall indicate that a wooden wall absorbs more sound energy which is reflected from the walls compared to a stiff acrylic glass wall.

Figure 4 shows the calculated factors C and C_A, which are the second part of the sound reduction index equations (1) and (2). In contrast to C, C_A considers the damping of the sound waves in air. The black lines are the values for acrylic glass and the grey ones for plywood. For lower frequency values (< 4 Hz), the damping factor does practically not affect C. At higher frequencies, it becomes increasingly important. However, since higher frequencies are considered in this study as well, it is not sufficient to neglect the damping factor. For all following calculations of R, C_A has therefore been used.
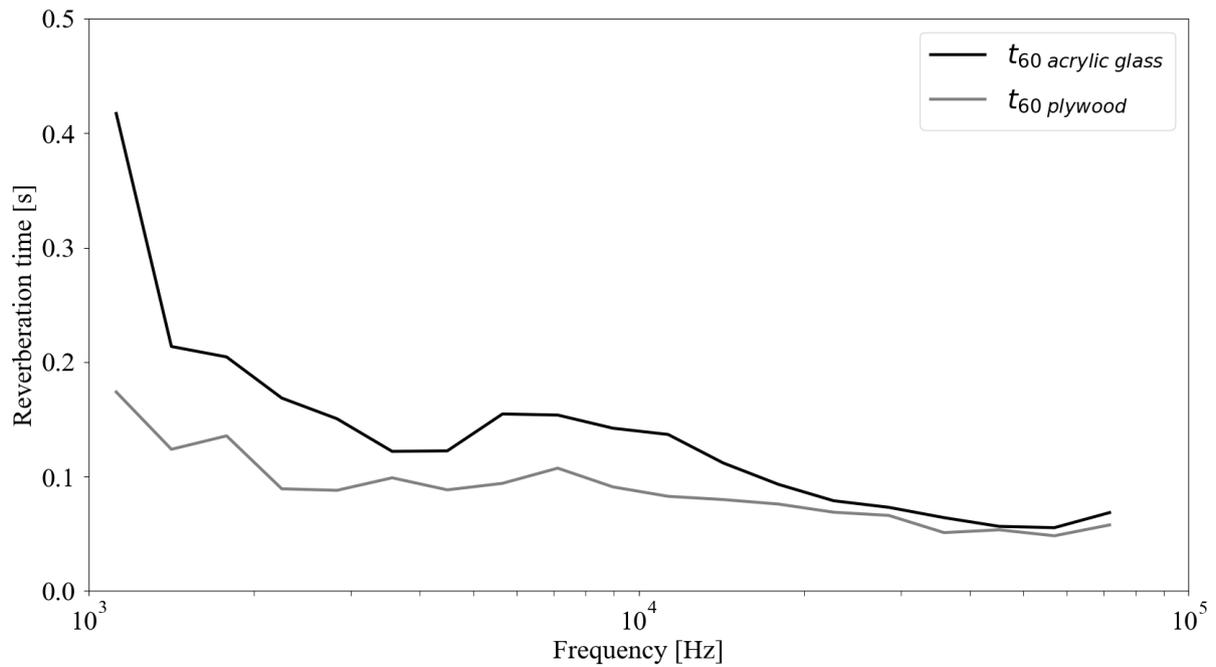
Figure 3: Reverberation times t_{60} in receiving room for acrylic glass and plywood
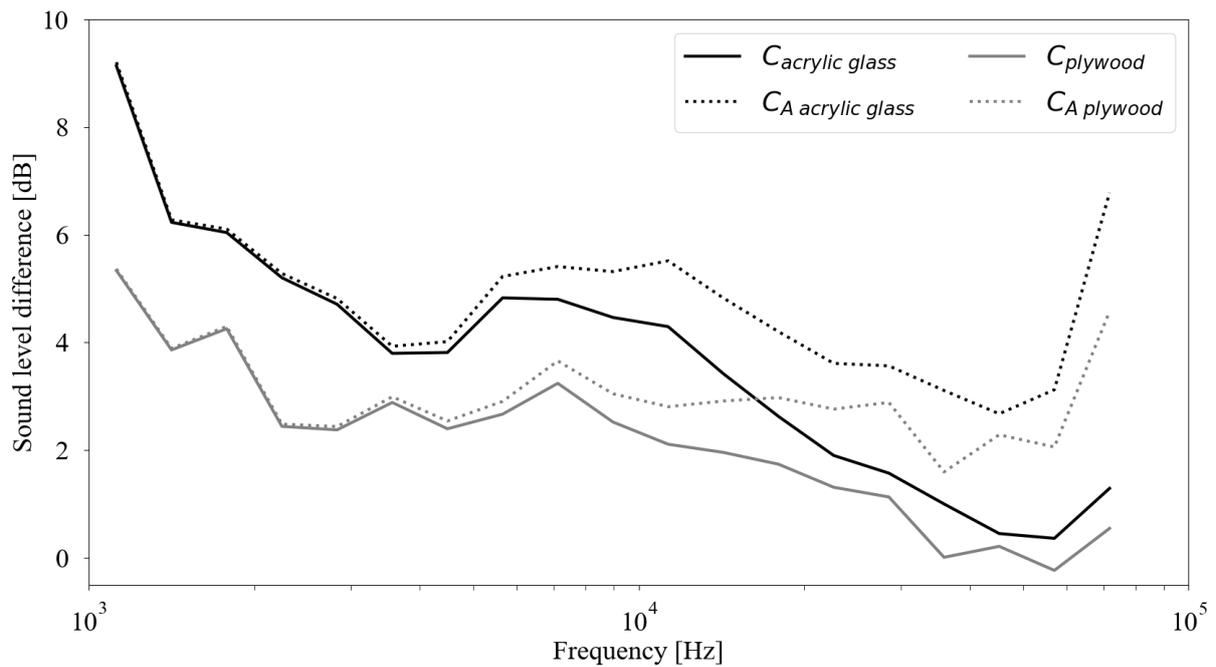

Figure 4: Factors C and C_A of the acrylic glass and the plywood wall at an ambient temperature of 24.3 °C and relative humidity of 23.0 %

3.2   Sound Reduction Index Measurements

In Figure 5 - 8, the sound reduction indexes *R* for acrylic glass and plywood walls are shown. The index indicates the sound transmission and absorption characteristics for these different wall materials at each frequency. In the upper part of each figure, four measured R-values as a function of frequency are illustrated. The solid lines are the measurements, which were taken

with a hole in the wall (4, 6, 8 or 10 mm). To be able to compare the reduction of R to a reference value, the same measurements were additionally performed with both wall materials under leak-proof conditions (dotted lines). These reference measurements are identical in all following figures.

In the same figures, the frequency dependence of the difference in R between the reference measurement and the measurement for each hole size is shown. This enables the identification of frequencies, where the output signal is predominantly affected by the hole size. If ΔR is negative, the sound reduction index of the measurement of a wall with a hole is lower compared to the same leak-proof wall. A lower sound reduction index indicates that more sound energy is transmitted at these frequencies.

The sound reduction index for plywood walls with no holes and for frequencies which are below 7.5 kHz is significantly lower compared to the same measurement with acrylic glass. For higher frequencies, the R-values for none of these two materials are dominant over a broad frequency band. Moreover, all following measurements show a sudden drop of the sound reduction index at a frequency of around 1.7 kHz, which is probably caused by a resonance.

The difference in sound reduction between measurements on walls with a hole and those with no hole grows with increasing hole diameter. This fact is presented in Table 1, where the mean differences of the sound reduction index are presented.
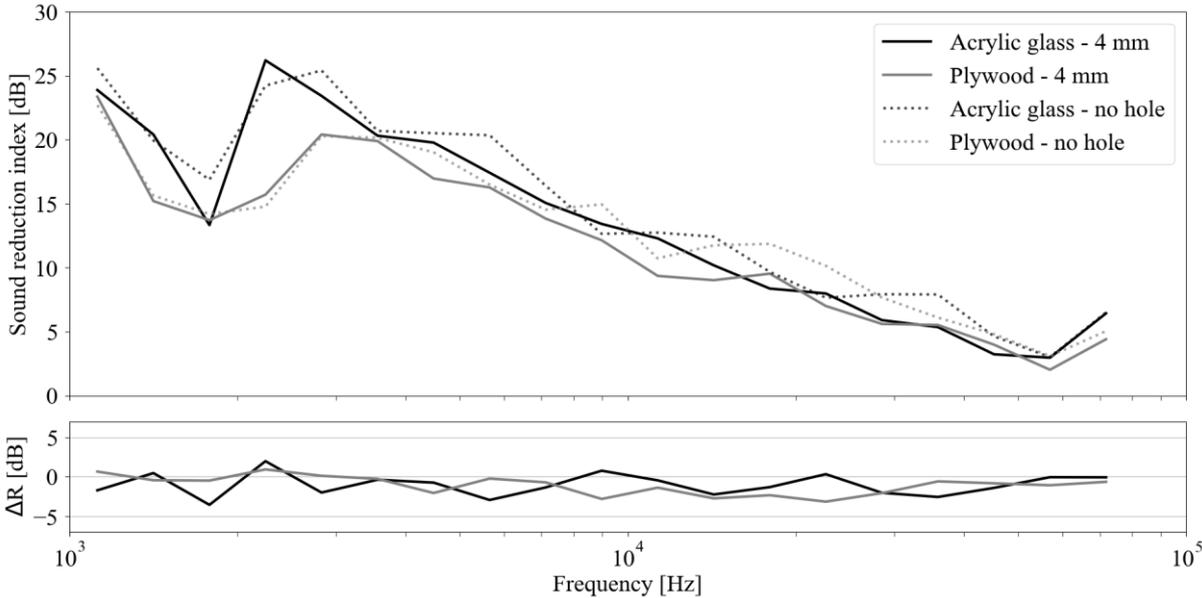

Figure 5: Sound reduction index R for measurements at walls with no holes (dotted lines) and walls with a 4 mm hole (solid lines in the upper graph) and differences of R from these two measurements (lower graph)
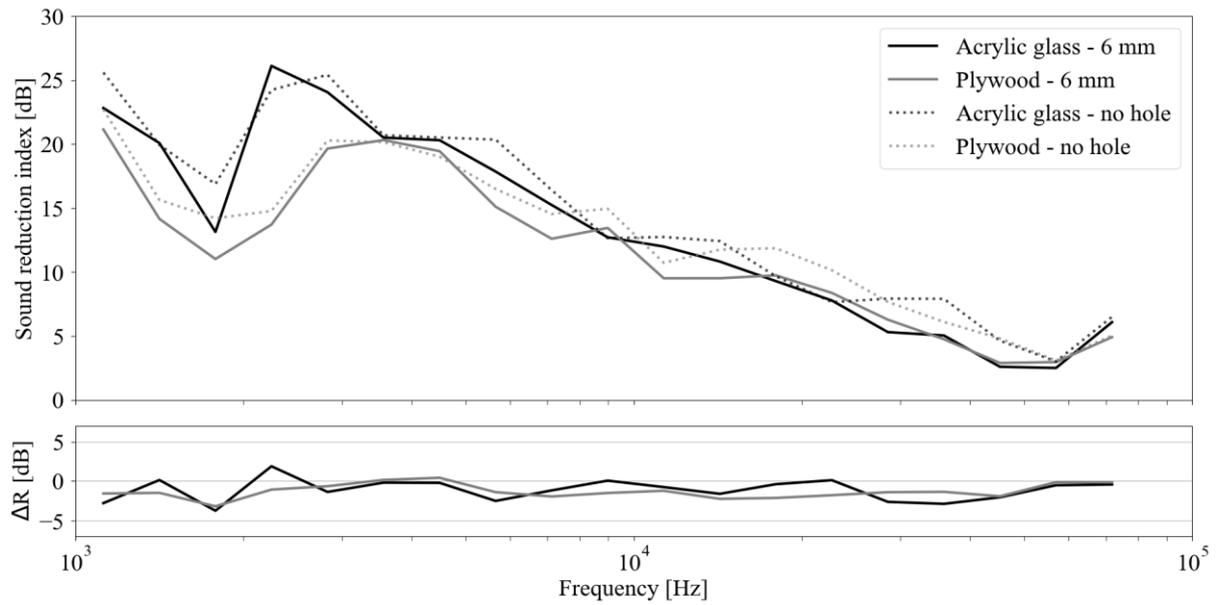
Figure 6: Sound reduction index R for measurements at walls with no holes (dotted lines) and walls with a 6 mm hole (solid lines in the upper graph) and differences of R from these two measurements (lower graph)
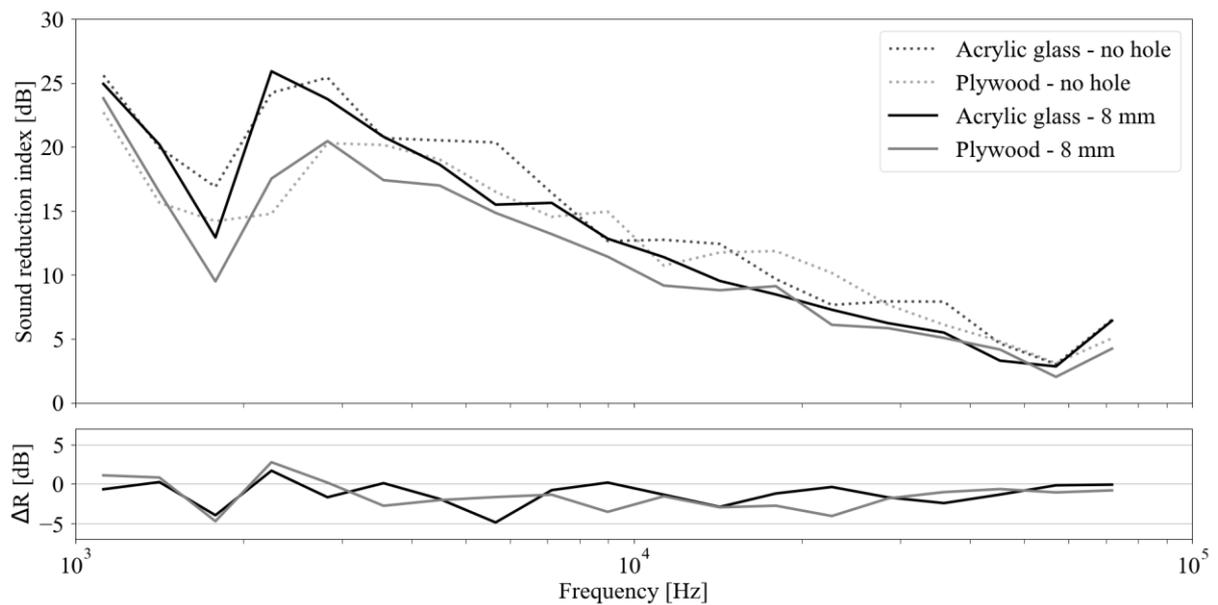

Figure 7: Sound reduction index R for measurements at walls with no holes (dotted lines) and walls with a 8 mm hole (solid lines in the upper graph) and differences of R from these two measurements (lower graph)
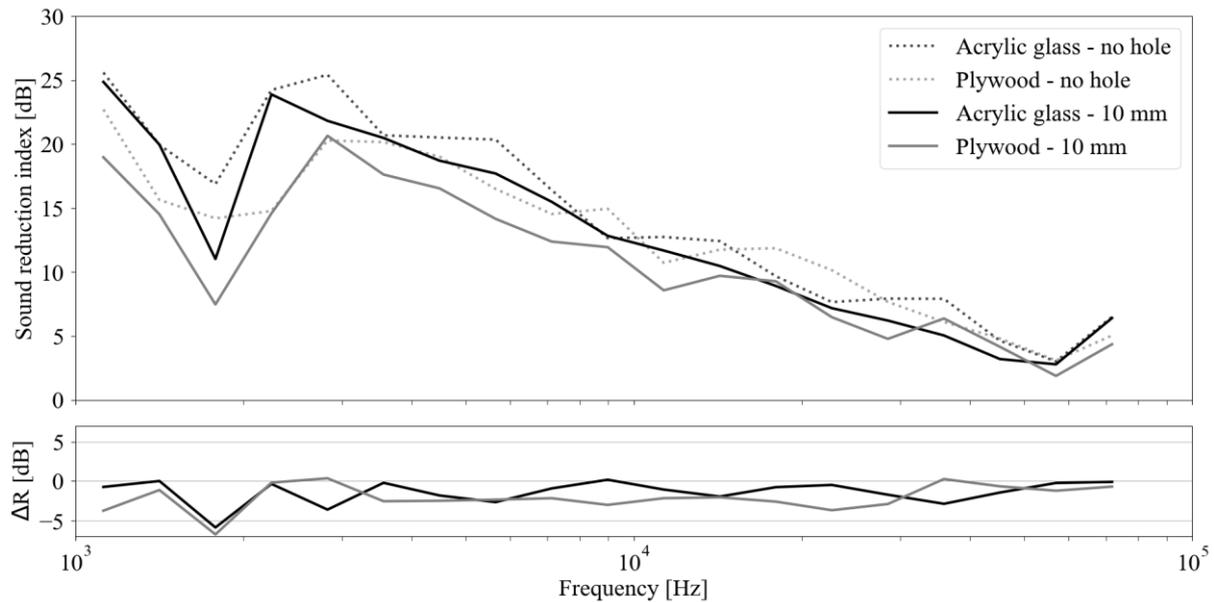
Figure 8: Sound reduction index R for measurements at walls with no holes (dotted lines) and walls with a 10 mm hole (solid lines in the upper graph) and differences of R from these two measurements (lower graph)

Table 1: The mean sound reduction index differences

	4 mm	6 mm	8 mm	10 mm
Acrylic Glass	-1.01	-1.10	-1.22	-1.39
Plywood	-1.05	-1.29	-1.48	-2.08

4 DISCUSSION

On average, over all frequencies, the sound reduction index decreases with increasing hole size. The differences are larger for the plywood walls compared to acrylic glass walls. This indicates that sound reduction and hole size may be correlated. A direct link between a specific frequency and the hole size could not be observed in these measurements.

5 CONCLUSIONS

In this paper, impulse responses over a wide frequency range have been used to determine the sound reduction indexes for an acrylic glass and a plywood wall with various hole sizes. It was possible to differentiate between leak-proof walls and walls with a hole. Furthermore, a distinction between different leakage sizes is possible. This technique may have the potential to locally determine leak sizes in walls, particularly if measurements are compared with nearby leak-proof wall parts as a reference.

In future work, similar measurements will be performed in a larger test bench, where simultaneous air infiltration measurements are possible. This will enable a better test of correlations between acoustic parameters and actual air infiltration. Additionally, more complex slit geometries and replicas of real building parts can be tested. Finally, the measurement procedure has to be validated with measurements at real building parts.

6 ACKNOWLEDGEMENTS

7 REFERENCES

Emmerich, S. J., McDowell, T. P., & Anis, W. (2005). *Investigation of the Impact of Commercial Building Envelope Airtightness on HVAC Energy Use* (US Department of Commerce, Technology Administration, National Institute of Standards and Technology, Ed.).

Estevam Schmiedt, J., Cerra, D., Dahlke, D., Dill, S., Ge, N., Göttsche, J., et al. (Eds.). (2017). *Remote sensing techniques for building models and energy performance studies of buildings*.

Farina, A. (Ed.). (2000). *Simultaneous measurement of impulse response and distortion with a swept-sine technique*.

International Energy Agency. (2013). *Technology Roadmap: Energy-efficient Buildings: Heating and Cooling Equipment,* OECD/IEA.

Lerch, R., Sessler, G., & Wolf, D. (2009). *Technische Akustik. Grundlagen und Anwendungen*. Berlin: Springer-Verlag.

Müller, G., & Möser, M. (2004). *Taschenbuch der Technischen Akustik* (3rd ed.). Berlin: Springer-Verlag.

Norm, DIN EN ISO 12354-1 (2017). *Building acoustics - Estimation of acoustic performance of buildings from the performance of elements - Part 1: Airborne sound insulation between rooms*. Berlin: Beuth Verlag.

Norm, DIN EN ISO 12569 (2018). *Thermal performance of buildings and materials - Determination of specific airflow rate in buildings - Tracer gas dilution method*. Berlin: Beuth Verlag.

Norm, DIN EN ISO 18233 (2006). *Acoustics - Application of new measurement methods in building and room acoustics*. Berlin: Beuth Verlag.

Norm, DIN EN ISO 9972 (2018). *Thermal performance of buildings – Determination of air permeability of buildings – Fan pressurization method*. Berlin: Beuth Verlag.

Norm, DIN EN ISO 3382-2 (2008). *Acoustics - Measurement of room acoustic parameters - Part2: Reverberation time in ordinary rooms*. Berlin: Beuth Verlag.

Norm, ISO 9613-1 (1993). *Acoustics - Attenuation of sound during propagation outdoors - Part 1: Calculation of the absorption of sound by the atmosphere*. Berlin: Beuth Verlag.

Sherman, M. H., & Chan, R. (2004). *Building Airtightness: Research and Practice,* Lawrence Berkeley National Laboratory.

TenWolde, A. (1994). Ventilation, humidity, and condensation in manufactured houses during winter. *ASHRAE Transactions, 100*(*1*), 103–115.

Wenmaekers, R. H. C., Hak, C. C. J. M., & Hornikx, M. C. J. (2014). The effective air absorption coefficient for predicting reverberation time in full octave bands. *The Journal of the Acoustical Society of America, 136*(*6*), 3063–3071. doi:10.1121/1.4901710